

# Topological Protection in Disordered Photonic Multilayers and Transmission Lines

D. M. Whittaker and R. Ellis

*Department of Physics and Astronomy, University of Sheffield, Sheffield S3 7RH, UK.*

(Dated: February 9, 2021)

The Su-Schrieffer-Heeger (SSH) model is the simplest example of a lattice with non-trivial topology. It supports mid-gap topologically protected states, whose energies are unaffected by disorder. We show that photonic multilayer structures provide an exact implementation of an SSH lattice, provided each layer has the same propagation thickness. From this, it follows that the cavity mode in a conventional semiconductor microcavity is a protected SSH mid-gap state. We demonstrate this experimentally using controlled disorder in a mathematically equivalent system, a radio frequency transmission line made from sections of coaxial cable with high and low impedances. We also show theoretically that transmission lines connected to form networks map onto topologically interesting lattices in higher dimensions.

The Su-Schrieffer-Heeger (SSH) model[1] is well known as the ‘toy’ system used to introduce the ideas of topology in solid state physics. It consists of a one dimensional chain of sites coupled by alternating weak and strong bonds. The SSH model has chiral symmetry, meaning that its spectrum is exactly symmetric when reflected about the middle of the band-gap. This symmetry is a prerequisite for non-trivial topology in one dimension. It provides topological protection for mid-gap states, so their energies are unaffected by variations in the parameters of the system.

Although the SSH model has its origins in polymers, there have been numerous attempts to construct photonic[2–6], acoustic[7, 8] and cold-atom[9] systems in order to implement the topological physics it describes. They all share the idea of creating a one-dimensional chain of resonators with alternating strong and weak couplings. However, this is not in itself enough to ensure chiral symmetry; it can be broken by effects such as on-site potentials, second nearest neighbour hopping and coupling to states not included in the manifold described by

the model. Such effects are unavoidable in these complex systems, so they do not exhibit exact chiral symmetry, and thus do not have the topology of the SSH model. We show that, by contrast, there is a class of very simple one-dimensional systems, described mathematically by transfer matrices, which possess exact chiral symmetry and map perfectly onto SSH chains. We consider two examples: multilayer photonic structures, where the layers have different refractive indices, and transmission lines with sections of different impedances. These structures have chiral symmetry if the propagation length of each layer, or line section, is identical.

A consequence of this mapping is that in semiconductor microcavity structures[10, 11], the cavity mode is an SSH mid-gap state. Disorder can be introduced into these structures, without breaking the chiral symmetry, by varying the refractive indices and layer thicknesses in a way which leaves the propagation lengths unchanged. They thus provide an ideal experimental platform for demonstrating the topological protection which is central to the SSH model. For the photonic case, we show numerically that when disorder is introduced in this way, the energy of the cavity mode is unaffected. We also demonstrate the protection experimentally in a mathematically analogous system of coaxial cables[14–16], where an ensemble of disordered structures can be constructed very easily by swapping in cables of different impedances.

It is important to distinguish the spectral chiral symmetry considered here from the spatial inversion symmetry possessed by all periodic bilayer structures. Inversion symmetry has been demonstrated to have topological consequences[12], which have been discussed in the context of photonic multilayers by Xiao et al[13], who show that it can be used to determine the conditions for finding a localised mode at an interface. However, this is not the topology of the SSH model. That requires chiral symmetry, which can also be found in multilayers, but only if the layers have the same propagation lengths. As we show, chiral symmetry can be maintained in the presence of disorder, while inversion symmetry is inevitably broken, so is not associated with topological protection.

The basic SSH model consists of a one dimensional chain of sites, all with the same energy. A particle can hop between adjacent sites, with hopping amplitudes alternating along the chain, as in Fig.1(a). The system

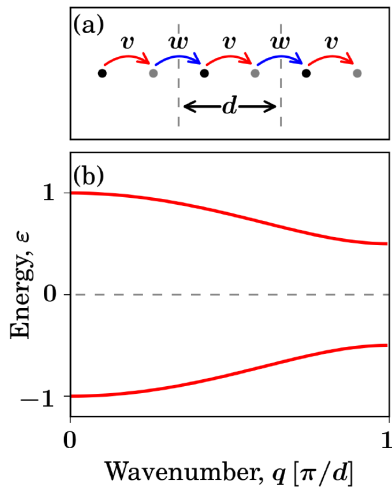


FIG. 1. (a) Schematic of part of an SSH lattice, showing the intra- and inter-cell hopping amplitudes,  $v$  and  $w$ . A single period, of length  $d$ , consists of two sites. (b) Band structure for the case  $v = 1/4$ ,  $w = 3/4$ . The band structure is symmetric about the dashed line at  $\epsilon = 0$ , the chiral point.

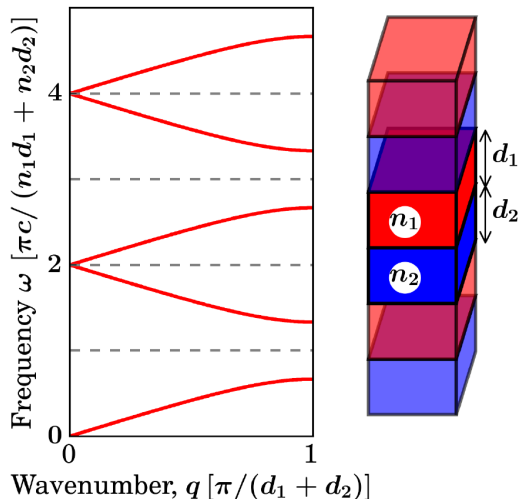


FIG. 2. Band structure of a Bragg stack. The schematic illustrates a section of the stack, which has a period of two layers with refractive indices  $n_1 = 3$  and  $n_2 = 1$ . The layer thicknesses satisfy the Bragg condition  $n_1 d_1 = n_2 d_2$ , giving chiral symmetry. The band structure is periodic in frequency, with period  $2\pi c/(n_1 d_1 + n_2 d_2)$ . The dashed lines show the chiral points; the bandstructure is exactly symmetric when reflected about these lines.

has two energy bands, shown in Fig.1(b), and also two distinct topologies, depending on which of the inter- and intra-cell hopping amplitudes is greater. An important property of the model is that the spectrum possesses chiral symmetry; it is exactly symmetric when reflected about the middle of the band-gap, which we will call the chiral point. The chiral symmetry is not restricted to the simplest case of alternating hopping amplitudes; it is present in any chain where there are only nearest neighbour hoppings, and the on-site energies are all the same. In such systems, energy states generally occur in pairs, which map onto each other when reflected about the chiral point. However, there are also special states, found at the chiral point, which map onto themselves, and are thus unpaired. In the SSH model, these are mid-gap states. They can occur at the end of a chain, or at an interface between two domains of different topology, created by repeating one of the hoppings in adjacent links. When the system parameters are varied, perhaps due to disorder, the energy of these states cannot change: if an unpaired state were to move from the chiral point, it would violate the chiral symmetry. Such states are said to be topologically protected.

## PHOTONIC MULTILAYERS

The photonic structures considered here consist of a one dimensional series of layers, characterised by a refractive index  $n$  and thickness  $d$ . The simplest such structure, the Bragg stack, is a periodically repeated bilayer, which has the bandstructure shown in Fig.2. By intro-

ducing defects in the periodicity, such as repeating layers, localised states can be created in the band gaps.

The simplest way to calculate the properties of such a layered structures is to use the transfer matrix formalism. The transfer matrix for a layer relates the amplitudes of the electric and magnetic fields,  $E$  and  $B$ , on either side of the layer. It is given by

$$\begin{pmatrix} E' \\ B' \end{pmatrix} = \begin{pmatrix} \cos(\omega\bar{d}/c) & in^{-1}\sin(\omega\bar{d}/c) \\ in\sin(\omega\bar{d}/c) & \cos(\omega\bar{d}/c) \end{pmatrix} \begin{pmatrix} E \\ B \end{pmatrix} \quad (1)$$

where  $\omega$  is the angular frequency,  $\bar{d} = nd$  is the propagation length of the layer and  $c$  is the speed of light in vacuum. Multiplying matrices for individual layers gives the transfer matrix for a structure, which can be used to calculate spectral properties such as transmission. The spectral symmetries of the transfer matrix follow directly from the periodicity and symmetries of the trigonometric functions in it. Apart from trivial phases, it is periodic in frequency, with period  $\pi c/\bar{d}$ , and symmetric about values of  $\omega$  which are integer multiples of  $\pi c/(2\bar{d})$ . If  $\bar{d}$  is the same for every layer, the transfer matrix for the whole structure will display these symmetries.

We next demonstrate that such chiral multilayers form exact implementations of an SSH chain. Consider a structure where each layer has the same propagation length,  $\bar{d}$ . Defining the fields  $E_i$  and  $B_i$  at the  $i^{\text{th}}$  interface, the transfer matrices can be used to eliminate the  $B_i$ , giving a relationship between the  $E_i$ :

$$n_{i-1,i} E_{i-1} + n_{i,i+1} E_{i+1} = (n_{i-1,i} + n_{i,i+1}) \cos(\omega\bar{d}/c) E_i \quad (2)$$

Here,  $n_{i,i+1}$  is the refractive index of the layer between the  $i^{\text{th}}$  and  $(i+1)^{\text{th}}$  interface. If we now define an ‘energy’  $\varepsilon = \cos(\omega\bar{d}/c)$  and scaled fields  $\tilde{E}_i = (n_{i-1,i} + n_{i,i+1})^{1/2} E_i$ , this becomes a tight-binding model,

$$t_{i-1,i} \tilde{E}_{i-1} + t_{i,i+1} \tilde{E}_{i+1} = \varepsilon \tilde{E}_i, \quad (3)$$

where the hopping amplitude is

$$t_{i,i+1} = \frac{n_{i,i+1}}{[(n_{i-1,i} + n_{i,i+1})(n_{i,i+1} + n_{i+1,i+2})]^{1/2}}. \quad (4)$$

This tight binding model has the form of an SSH chain: there are only nearest-neighbour hoppings and the on-site energies are all zero.

When applied to the case of a conventional bilayer Bragg stack, Eq.(4) gives two values for the hopping amplitudes,  $n_1/(n_1 + n_2)$  and  $n_2/(n_1 + n_2)$ , for the layers with index  $n_1$  and  $n_2$ , respectively. The tight binding system is then identical to the simplest SSH model. If the layer propagation lengths are commensurate rather than identical, it is necessary to divide the layers into sub-units of equal thickness. The tight binding model then has more than two layers per unit cell, corresponding to generalised SSH systems, such as the SSH-4 model[17, 18].

A conventional microcavity structure is made by joining two Bragg stacks with the same termination, giving

a defect with twice the thickness of a normal layer. The doubled layer corresponds to two hops with the same amplitude, so this is an exact experimental realisation of the interface between SSH domains of different topology. The cavity mode is found at the mid-gap chiral point, and corresponds to the topologically protected interface state. This means that its frequency should be unaffected by disorder consisting of variations in the refractive indices of the layers of the structure. However, chiral symmetry needs to be maintained, so the propagation length,  $\bar{d} = nd$ , of each layer must be kept constant, by adjusting its thickness when the refractive index is changed.

In Fig.3, we show transmission spectra, calculated using the transfer matrix method, which demonstrate topological protection for a microcavity in which the refractive index of each layer is varied randomly, adjusting the thickness to maintain the chiral condition. We consider two structures, with and without a chiral symmetry point in the lowest gap. The first (Fig.3(a)) is a conventional cavity satisfying the Bragg condition  $n_1d_1 = n_2d_2$ , giving a chiral point in the middle of the gap, so the cavity mode is topologically protected. The second structure (Fig.3(b)) is more complicated. The transmission thickness of a period,  $n_1d_1 + n_2d_2$  is constant, but the ratio of high to low index material is reversed at the interface: on one side  $n_1d_1 = 3n_2d_2$ , while on the other  $n_2d_2 = 3n_1d_1$ . These mirrors have identical bandstructures and the interface supports a cavity mode in the middle of every gap. However, the structure maps onto an SSH-4 model, so there is no chiral point in the first gap, and no topological protection. The difference is evident in the spectra: for the chiral case, there is absolutely no change in the energy of the cavity peak, while without the protection, each instance of the disorder gives a distinct peak. In Fig.3(c), we plot the electric field profile of the mode for the chiral case. There is a different profile for each instance of the disorder, but in all cases the field goes to zero at alternate interfaces. This relates to the form of the protected state in SSH systems, which has zero amplitude on alternate sites.

The main factor determining how closely exact chiral symmetry can be approached is likely to be the accuracy of the fabrication, ensuring that the propagation length of each layer is the same. The description in terms of a constant, real refractive index also needs to be considered. The frequency dispersion of the index is not really an issue, because the topological protection only requires the matching to be exact at the chiral point. Absorption, corresponding to a complex refractive index  $n + i\kappa$ , can break the chiral symmetry. However, it produces fractional energy shifts  $\sim (\kappa/n)^2$ , which can be made very small with appropriate material choices. Furthermore, a mode of quality factor  $Q$ , without absorption, will also be weakened to the point where it becomes unobservable when  $\kappa/n \sim 1/Q$ , so the maximum detectable shift due to absorption will be of order of the linewidth divided by  $Q$ .  $Q$  values of thousands are achievable in semiconductor microcavities, so this is a small effect.

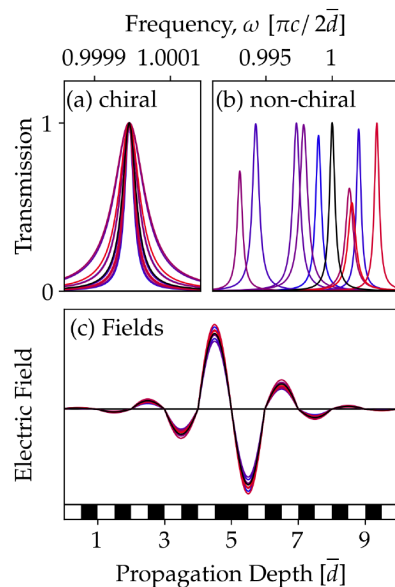


FIG. 3. Topological protection for a chiral multilayer photonic structure. (a) and (b) show calculated transmission spectra, in the frequency range around the middle of the first band-gap, for a cavities created by joining two disordered Bragg mirrors. Each mirror consists of five periods, terminated at the interface with a high index layer. The structures are designed (see text) so that both have a mid-gap cavity mode; in (a) this corresponds to a chiral point, making the mode topologically protected, while in (b) the chiral point is in a higher gap, so there is no protection. The colours correspond to ten instances of disorder, in which the refractive index in each layer is varied randomly by  $\pm 20\%$ , from the nominal values of  $n_1 = 3$  and  $n_2 = 1$ , while the layer thickness is adjusted to keep the propagation length  $\bar{d} = nd$  constant. The black curves are reference spectra without disorder. (c) shows electric field profiles for the protected mode in (a), plotted as a function of the optical depth, so the layer interfaces, shown in the black and white bar, coincide for all structures.

## TRANSMISSION LINE STRUCTURES

The chiral and topological properties discussed above follow from the form of the transfer matrices which describe the structures. Similar mathematics occurs in other situations where waves are one-dimensional, such as acoustic waves in multilayers and waves on strings. Hence, it should be possible to find the physics of topological protection in these systems. We shall consider the propagation of radio-frequency signals in coaxial cable transmission lines. For an ideal, lossless, cable, the transfer matrix relates the voltage,  $V$ , and current,  $I$  at either end, according to

$$\begin{pmatrix} V' \\ I' \end{pmatrix} = \begin{pmatrix} \cos(\omega d/v) & iZ \sin(\omega d/v) \\ iZ^{-1} \sin(\omega d/v) & \cos(\omega d/v) \end{pmatrix} \begin{pmatrix} V \\ I \end{pmatrix}, \quad (5)$$

where the impedance  $Z = \sqrt{L/C}$ , and the propagation velocity  $v = 1/\sqrt{LC}$ , with  $L$  and  $C$  the inductance and capacitance per unit length. This has the same form as Eq.(1), so exact analogues of photonic multilayer struc-

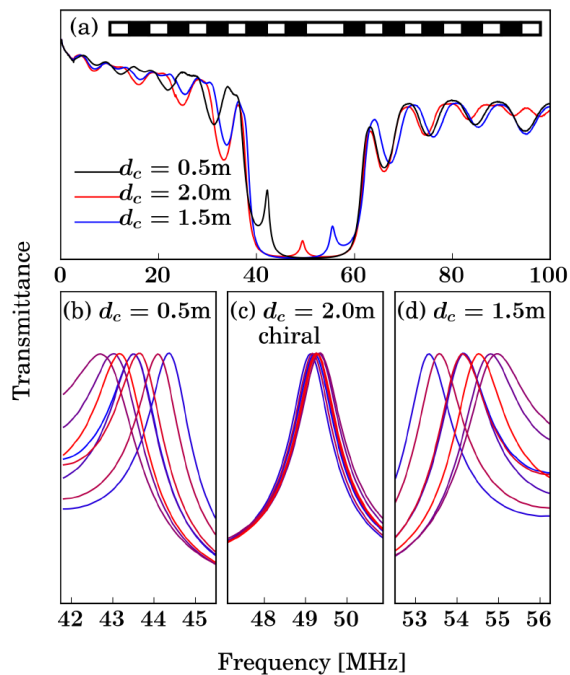


FIG. 4. Experimental transmittance spectra for cavity structures made from coaxial cables. (a) spectra for structures without disorder, shown schematically in the inset. Each has two chiral mirrors, made from five repeats of a pair of cables with impedances  $50\Omega$  (white) and  $93\Omega$  (black), surrounding a  $50\Omega$  section defining the cavity. The physical lengths of the  $50\Omega$  and  $93\Omega$  cables in the mirrors are  $1.0\text{m}$  and  $1.24\text{m}$  respectively, giving the same propagation lengths. Three cavity lengths,  $d_c$ , are used: for  $d_c = 2.0\text{m}$ , the propagation length is double that of the mirror layers, so the chiral symmetry is maintained, while for  $d_c = 0.5\text{m}$  and  $1.5\text{m}$ , it is broken. The band-gap corresponds to the strong dip in transmission, between about  $40$  and  $60$  MHz, containing the peak due to the cavity mode. (b)-(d) show normalised spectra, in the region of this mode, for eight different structures with disorder, where half of the  $93\Omega$  sections are selected randomly and replaced with  $75\Omega$  cables. Identical mirrors are used with each cavity, indicated by the line colours. In the chiral case, (c), the disorder has very little effect on the mode frequency, demonstrating that it is topologically protected

tures can be constructed by joining sections of transmission line with different impedances[14–16].

Transmission lines made from coaxial cable sections with the same propagation length  $\bar{d} = dc/v$ , are a convenient system for demonstrating the topological protection discussed above. It is straightforward to make an ensemble of instances of disorder by swapping in sections of cable with different impedances. Transmittance spectra for cavities constructed in this way are shown in Fig.4. We consider three cavity structures: in each case, the mirrors consist of a repeated chiral bilayer, but in one the chiral symmetry is maintained as the cavity is formed by repeating one of the low impedance layers ( $d_c = 2.0\text{m}$ ), while the other two deliberately break the symmetry, with cavities of different lengths. When disorder is introduced into the mirrors, the mode in the chiral cavity undergoes very little change in frequency, demonstrating

the topological protection. By contrast, the non-chiral structures show a broad spread in frequency between the different instances of the disorder. However, even in the non-chiral structures, the mirrors on either side of the cavity layer retain their chiral symmetry. This accounts for the near reflection symmetry between equivalent spectra in Fig.4(b) and (d): the cavity modes are approximately equidistant in frequency from the chiral point, so they experience similar changes in mirror reflectivity for a given instance of the disorder.

With transmission lines, we can go further than simple one-dimensional chains, since more than two cables can meet at a junction. We then have a network rather than a simple transmission line. When the propagation lengths,  $\bar{d}$ , of all the cables is the same, our result, Eq.(2), generalises to

$$\sum_j Z_{ij}^{-1} V_j = \sum_j Z_{ij}^{-1} \cos(\omega\bar{d}/c) V_i \quad (6)$$

where the sums are over the nearest neighbours of site  $i$ , to which it is directly connected. A similar result has been derived by Zhang and Sheng[19], for microwave waveguide networks. With the equivalent rescaling and identification of  $\varepsilon = \cos(\omega\bar{d}/c)$ , this again looks like a tight binding model. Provided any loops have an even number of nodes, this network will have chiral symmetry, and so potentially non-trivial topology. In such a network the spatial positioning of sites is unimportant, the only relevant consideration being how they are connected. Hence lattices can be fabricated which are impossible under the physical constraints of three dimensional space[20, 21] and Euclidean geometry[22]. Transmission line structures can also be seen as a bridge between photonic systems and topological circuits[23, 24]. It is natural to combine transmission lines with discrete electronics located at the nodes, providing, for example, gain and loss or nonlinearity. This would extend the range of models which can be studied to include PT symmetric[25] and nonlinear systems.

To conclude, we have shown that commensurate photonic multilayers provide exact implementations of SSH chains, with perfect chiral symmetry. A Bragg stack, with equal propagation lengths for the layers, corresponds to the basic SSH model, and conventional microcavity modes are the interface states between regions of different topology. We have demonstrated this experimentally using coaxial transmission lines, a mathematically analogous system, where we show that the cavity mode is topologically protected against a particular class of disorder. Finally, we have shown that the same mathematics works in transmission line networks, suggesting that they are a promising platform for more general studies of topological physics.

We wish to thank E. Chekhovich for help with setting up the experiment.

- 
- [1] W. P. Su, J. R. Schrieffer and A. J. Heeger, *Phys. Rev. Lett.* **42**, 1698 (1979).
- [2] T. Ozawa, H. M. Price, A. Amo, N. Goldman, M. Hafezi, L. Lu, M. C. Rechtsman, D. Schuster, J. Simon, O. Zeitler and I. Carusotto, *Rev. Mod. Phys.* **91**, 015006 (2019).
- [3] N. Malkova, I. Hromada, X. Wang, G. Bryant and Z. Chen, *Opt. Lett.* **34**, 1633 (2009).
- [4] C. Poli, M. Bellec, U. Kuhl, F. Mortessagne and H. Schomerus, *Nat. Commun.* **6**, 6710 (2015).
- [5] P. St-Jean, V. Goblot, E. Galopin, A. Lemaître, T. Ozawa, L. Le Gratiet, I. Sagnes, J. Bloch and A. Amo *Nat. Photonics* **11**, 651 (2017)
- [6] F. Bleckmann, Z. Cherpakova, S. Linden and A. Alberti, *Phys. Rev.* **B96**, 045417 (2017).
- [7] X Li, Y. Meng, X. Wu, S. Yan, Y. Huang, S. Wang and W. Wen *Appl. Phys. Lett.* **113**, 203501 (2018).
- [8] M. Esmann, F. R. Lamberti, A. Lemaître and N. D. Lanzillotti-Kimura, *Phys. Rev. B* **98**, 161109(R) (2018).
- [9] M. Atala, M. Aidelsburger J. T. Barreiro, D. Abanin, T. Kitagawa, E. Demler and T. Bloch *Nat. Phys.* **9**, 795-800 (2013).
- [10] C. Weisbuch, M. Nishioka, A. Ishikawa and Y. Arakawa, *Phys. Rev. Lett.* **69**, 3314 (1992).
- [11] M. S. Skolnick, T. A. Fisher and D. M. Whittaker, *Semi-conduct. Sci. Technol.* **13**, 645-669 (1998).
- [12] J. Zak, *Phys. Rev. Lett.* **62** 2747 (1989).
- [13] Meng Xiao, Z. Q. Zhang and C. T. Chan, *Phys. Rev. X* **4**, 021017 (2014).
- [14] G. J. Schneider, S. Hanna, J. L. Davis and G. H. Watson, *J. Appl. Phys.* **90**, 2642 (2001).
- [15] J. N. Munday and W. M. Robertson, *Appl. Phys. Lett.* **83**, 1053 (2003).
- [16] M. M. Sánchez-López, J. A. Davis and K. Crabtree, *Am. J. Phys.* **71**, 1314 (2003).
- [17] M. Maffei, A. Dauphin, F. Cardano, M. Lewenstein and P. Massignan, *New J. Phys.* **20** 013023 (2018).
- [18] D. Xie, W. Gou, T. Xiao, B. Gadway and B. Yan, *NPJ Quantum Inf.* **5**, 55 (2019).
- [19] Z. Q. Zhang and P. Sheng, *Phys. Rev. B* **49**, 83 (1994).
- [20] S. Ryu, A. P. Schnyder, A. Furusaki and A. W. W. Ludwig, *New J. Phys.* **12**, 065010 (2010).
- [21] S.-C. Zhang and J. Hu, *Science* **294**, 823 (2001).
- [22] A. J. Kollár, M. Fitzpatrick and A. A. Houck, *Nature* **571**, 45 (2019).
- [23] J. Ningyuan, C. Owens, A. Sommer and D. Schuster and J. Simon *Phys. Rev. X*, **5**, 021031 (2015).
- [24] C. H. Lee, S. Imhof, C. Berger, F. Bayer, J. Brehm, L. W. Molenkamp, T. Kiessling and R. Thomale, *Commun. Phys.* **1** 39 (2018).
- [25] R. El-Ganainy, K. G. Makris, M. Khajavikhan, Z. H. Musslimani, S. Rotter and D. N. Christodoulides, *Nat. Phys.* **14** 11 (2018).